Advances in Safety, Reliability and Risk Management – Bérenguer, Grall & Guedes Soares (eds)
© 2012 Taylor & Francis Group, London, ISBN 978-0-415-68379-1

A dynamic level 2 PRA using ADAPT-MELCOR

D.M. Osborn, D. Mandelli, K. Metzroth, T. Aldemir & R. Denning
Nuclear Engineering Program, The Ohio State University, Columbus, OH, US

U. Catalyurek
Biomedical Informatics, The Ohio State University, Columbus, OH, US

ABSTRACT: This paper discusses the work which has been conducted for a Level 2 Probabilistic Risk Assessment (PRA) Station Blackout Scenario using a dynamic event tree analysis methodology. The methodology is implemented using the Analysis of Dynamic Accident Progression Trees (ADAPT) software. This work is an extension of past MELCOR-ADAPT dynamic PRA in which additional parameters are considered including creep rupture distributions for carbon steel (CS), stainless steel (SS), and Inconel (IS) for the pressurizer (SS), steam generators (IS), and for multiple reactor coolant loops (CS and SS). Additionally, multiple Safety Relief Value (SRV) failures are considered for per-demand failure, and high temperature cycling failure probability distributions. An updated containment fragility curve was incorporated using data from NUREG/CR-5121 and NUREG/CR–6920. This work allows for better insight into the potential timing differences for creep rupture at various locations in the reactor coolant system and investigates multiple SRV failures.

1 INTRODUCTION

1.1 *Problem description*

The current approach to Level 2 PRA using the conventional event/fault-tree methodology requires pre-specification of event order occurrence which may vary significantly in the presence of uncertainties (Catalyurek et al. 2010). Manual preparation of input data to evaluate the possible scenarios arising from these uncertainties and their execution using serial runs may lead to errors from faulty/incomplete input preparation as well as to infeasible run times. A methodology has been developed for Level 2 analysis using dynamic event trees (DETs) that removes these limitations with systematic and mechanized assessment of possible scenarios arising from the uncertainties (Catalyurek et al. 2010). The methodology is implemented using the Analysis of Dynamic Accident Progression Trees (ADAPT) software which has been linked (Hakobyan et al. 2008) to the MELCOR code (Gauntt et al. 2005).

1.2 *Objective and scope*

The objective of this research is to extend the ADAPT (Catalyurek et al. 2010; Hakobyan et al. 2008) methodology to a full dynamic Level 2 PRA in which additional parameters are considered. This work uses MELCOR (Gauntt et al. 2005) as a reactor plant simulator. The DETs will cover all possible scenarios in the user-specified discretized uncertainty space and will be generated/evaluated in a mechanized fashion using distributed computer and intelligent scheduling to reduce analysis time and cost.

The MELCOR code was developed by Sandia National Laboratories (SNL) for the U.S. Nuclear Regulatory Commission (NRC) to model the progression of accidents in a light water reactor. A broad spectrum of accident phenomena in both pressurized water reactors (PWR) and boiler water reactors (BWR) are treated within the code. MELCOR can estimate the fission product source term as a result of containment breach or containment bypass.

For this work, a series of MELCOR input decks for a 3-loop PWR with a steam supply system and a sub-atmospheric dry containment experiencing a station blackout (SBO) is investigated. The availability of AC electrical power is essential for the safe operation and accident recovery of a commercial nuclear power plant. Offsite power normally supplies this essential AC power. If the plant loses offsite power, the onsite emergency diesel generators can provide a reliable emergency AC power source. A total loss of AC power in which both offsite and onsite AC power sources are unavailable is called a station blackout (USNRC, 2005).

The ADAPT code was developed by the Ohio State University (OSU) as part of a SNL

Laboratory Directed Research and Development project to generate dynamic event trees. A system simulator such as MELCOR can be linked with ADAPT to determine possible scenarios based on the branching and stopping rules provided by the user. ADAPT can keep track of scenario likelihoods and graphically display the DETs, as well as all simulator output as a function of time.

2 COMPUTER CODE OVERVIEW

2.1 *MELCOR*

MELCOR was developed by SNL for the NRC to model the progression of accidents in a light water reactor. A broad spectrum of accident phenomena in both PWRs and BWRs are treated within the code. MELCOR is divided into 20 different packages and an execution primer. All of these packages are coupled within the code to model major reactor plant systems. The codes response to accident conditions include but are not limited to (Gauntt et al. 2005):

- Thermal-hydraulic response of the primary reactor coolant system, the reactor cavity, the containment, and the confinement buildings,
- Core uncovering, fuel heat up, cladding oxidation, fuel degradation, and core material melting and relocation,
- Heat up of reactor vessel lower head from relocated fuel materials and the thermal mechanical loading and failure of vessel lower head and transfer of core materials to the reactor vessel cavity,
- Core-concrete attack and ensuing aerosol generation,
- In-vessel and ex-vessel hydrogen production, transport, and combustion,
- Fission product release, transport, and deposition,
- Behavior of radioactive aerosols in the reactor containment building and,
- Impact of engineered safety features on thermal-hydraulic and radionuclide behavior.

The MELCOR model uses a 'control volume' approach for describing and combining reactor plant systems. There are no specific 'nodes' that a user must incorporate and thus allows for a greater degree of freedom. With this in mind it is possible for MELCOR to provide a detailed and unique reactor plant model for any type of PWR or BWR and has been even proven to successfully model Russian VVER and RMBK-reactor classes (Gauntt et al. 2005).

The first part of the MELCOR execution is called MELGEN. MELGEN provides a starting point for MELCOR. The majority of the initial conditions are specified, processed, and checked for execution errors in MELGEN. Upon execution of MELGEN, a restart file for MELCOR is written. The MELCOR code is then executed using this restart file and advances the accident scenario through predetermined time steps until a prespecified end time is achieved.

As part of the MELCOR/MELGEN output, a plot file (.PTF) is created. The MELCOR output variables are written to this plot file at predetermined time intervals set by the user. The plot file can be converted into a text file which can be read by post processing analysis described in Section 2.3 of this work. Figure 1 provides a graphic overview of the MELCOR code and file relations.

The MELCOR version used for this research is Version 1.8.6 which was released in September 2005. For further information into the MECLOR modeling packages, refer to NUREG/CR-6119 (Gauntt et al. 2005).

2.2 *ADAPT*

ADAPT has a distributed computing architecture: a simulator driver, centralized server, a database storage area, and a Graphic User Interface (GUI) based client side software. Figure 2 provides a schematic overview of the ADAPT computational infrastructure. The ADAPT framework is an open architecture that will allow for easy replacement of the component modules, and algorithms used in those components (Catalyurek, 2010). The ADAPT system components assume that for a single event tree, a single simulator is used to follow the transient.

With the use of a simulator agnostic *Driver* (Fig. 3), ADAPT currently provides means to process the output of a single simulator and edit/modify (Apply Edit Rules in Fig. 3) input files for dynamic branching. The Driver of the simulator (for this work, MELCOR) will read input, conduct

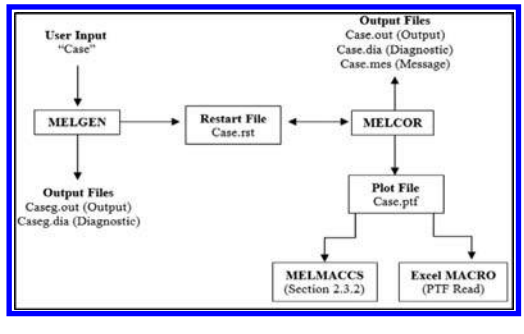

Figure 1. MELCOR code and file relation.

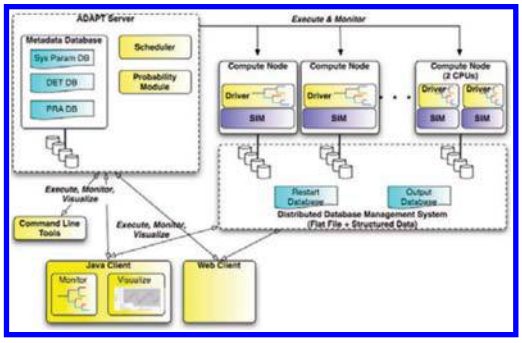

Figure 2. ADAPT system architecture (Catalyurek, 2010).

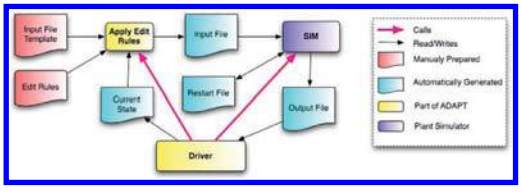

Figure 3. ADAPT driver (Catalyurek, 2010).

check-pointing, allow users to define stopping conditions, and utilize output to detect stopping conditions. The Driver also allows for a user-defined edit-rules file to be created. Figure 3 provide an illustration of the Driver's workflow interactions with a plant simulator.

ADAPT maintains a distributed database. ADAPT has the capability to access the DETs and the input and output files of the simulations, and the metadata. ADAPT also maintains basic statistics within the metadata. ADAPT allows the use of XML schemas to describe the metadata schema and create a generic framework which will allow for the design and deployment of multiple schemas for the multiple simulator drivers (Catalyurek, 2010). The ADAPT database system can efficiently process analysis queries such as plotting system variables which may require accessing multiple output files stored over multiple nodes.

ADAPT has a Java based GUI as a client tool. The client tool can allow a user to submit new initiation events, monitor the generation of DETs, check-point a running experiment, restart a check-pointed experiment, and allow the functionality of analyzing simulation results. The client tool also has the capability to differentiate between completed branches, insignificant branches, and abnormally terminated branches. The client tool is accessed through a web portal. Figure 4 provides an example of generated DETs as viewed through the web portal.

Figure 4. ADAPT client tool.

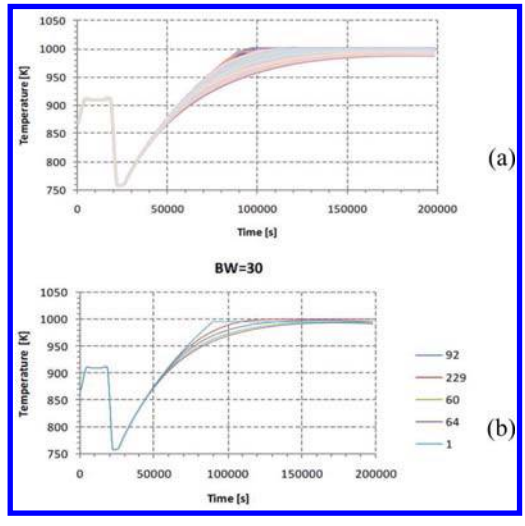

Figure 5. Scenario reduction: (a) full set, (b) reduced set (Mandelli et al. 2010). The numbers in (b) indicate the number of scenarios in each cluster.

2.3 *Post-processing*

Since the amount of data to be produced from a dynamic PRA may be difficult to analyze, the concept of 'data mining' provides a methodology to extract useful information. A post-processing tool has been developed by OSU to data mine DETs by using the mean-shift methodology to cluster scenarios (Mandelli et al. 2010). The scenarios are aggregated according to information on system components (valves failed open or pumps fail) and system process variables such as pressure and temperature in the reactor coolant system. The clustering of scenarios accomplishes two tasks (Mandelli et al. 2010):

1. Identify the scenarios that have 'similar' behaviors (i.e. identify the most evident clusters), and
2. Assign each scenario to a cluster (i.e. classification).

This methodology uses a non-parametric iterative mode-seeking procedure. The algorithm uses a hyper-dimensional sphere centered about a generic mean point with the radius of the sphere being called the bandwidth (BW) as a measure of similarity of scenarios. Figure 5 provides an example of how this methodology reduces the DET scenarios from 446 individual scenarios (Figure 5a) to 5 clusters with representative scenarios (Figure 5b). The process allows a more manageable analysis of scenarios and better visualization of the data. Figure 5 shows that this methodology can still allow for single outlier scenarios to be differentiated from those scenarios that are more similar.

3 UNCERTAINTY PARAMETERS

3.1 *Creep rupture*

Building upon past Level 2 dynamic PRA experiments (Hakobyan et al. 2008; Hakobyan et al. 2006a,b), the creep rupture distributions for the stainless steel in the surge line, the stainless steel in the hot leg for loops A & C, the carbon steel in the hot leg loops A & C, and the Inconel in the steam generator U-tubes for Loops A & C are considered. Figure 6 provides the nodalization of the 3-loop PWR for the MELCOR simulation. As shown in Figure 6, the pressurizer (modeled as one control volume) is attached to Loop C of the reactor coolant system.

The primary system loops are modeled for natural circulation. As a result the hot leg control volumes consist of four volumes rather than two as shown in Figure 6. This allows for the MELCOR model to simulate the counter-current flow

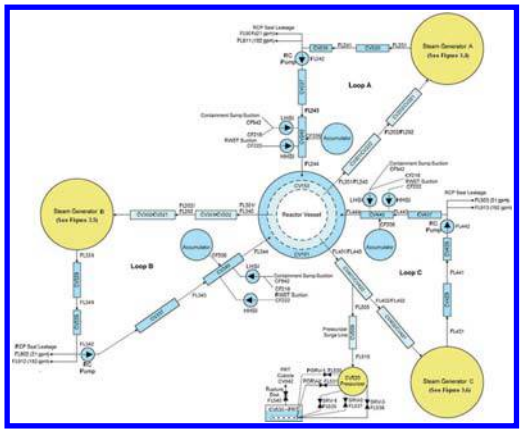

Figure 6. Reactor coolant loops.

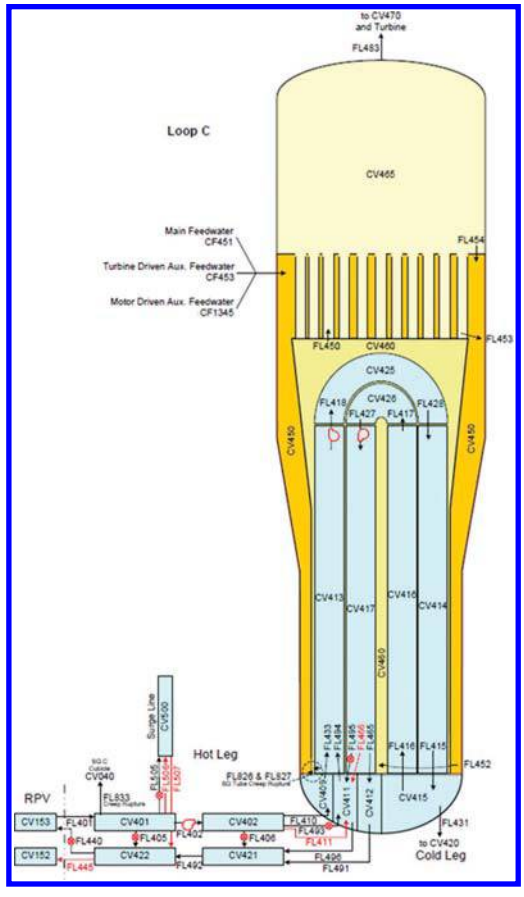

Figure 7. Nodalization of hot leg loop C.

that can occur during some accident transients. Figure 7 provides an example of the control volumes and flow paths needed for natural circulation. The red flow arrows, pressure adjustments (red pumps), and open/close pathways (⊗) are enabled only when natural circulation conditions are met. Figure 7 also shows the primary (blue control volumes) and secondary sides of the steam generator. The inlet plenum and tubes are broken down into smaller control volumes to better mdel counter-current flow condidtions during an accident.

Equation 1 shows the creep-rupture failure model in which time to rupture, t_R, is determined with the following (Gauntt et al. 2005):

$$t_R = 10^{\frac{P_{LM}}{T} - C} \tag{1}$$

where t_R = time to rupture (seconds); P_{LM} = Larson-Miller parameter; T = temperature (K); and C = material property.

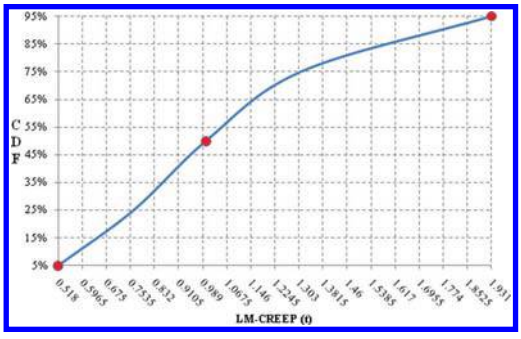

Figure 8. Creep rupture parameter distribution.

Figure 8 shows the distribution of the creep rupture parameter. This parameter is monitored by a MELCOR control function, LM-CREEP(t) which uses the Larson-Miller correlation in Equation 1 to predict rupture. Usually when LM-CREEP(t) = 1, MELCOR assumes that creep rupture occurs. However, Equation 1 originates from a fitting of the experiment data and hence has uncertainties associated with the dispersion of the data. The uncertainty can be accomodated for by: a) determining a cumulative distribution function (Cdf) that represents the spread of the data around the fitting, b) selecting points on the Cdf, c) choosing a rupture parameter that corresponds to the probability point, and, d) creating a scenario branch when this value is reached (i.e. rupture occurs or rupture does not occur).

The point selection scheme shown in Figure 8 has been used in past work (Hakobyan et al. 2008; Hakobyan et al. 2006 a,b; Rutt et al. 2006) and has been created using expert elicitation and experimenal data for stainless steel, carbon steel, and Inconel creep rutpure. For this research, only the 5%, 50%, and 95% creep rupture parameters corresponding to LM-CREEP = 0.518, 1.00, and 1.931, respectively were used. Although this course treatment results in an observable truncation error (Metzroth et al. 2010) within the framework of other uncertainties, the benefit of greater accuracy must be weighted against the cost of additional run time.

All reactor coolant piping is made of stainless steel. In fact, all steel in contact with primary coolant water is either stainless steel or clad with stainless steel. There is no carbon steel in the hot legs. However there is a narrow safe zone where the stainless steel hot leg connects with the reactor presure vessel nozzle. At this location, there is a thin stainless steel cladding that is surrounded by a field weld made of carbon steel. Thus this safe zone is modeled using carbon steel creep rupture parameter correlations.

3.2 *Safety relief valves (SRVs)*

All three steam generators A, B, and C have SRVs (SRV-A, SRV-B, and SRV-C respectively) as well as the pressurizer (SRV-P). The MELCOR model is set up to cause these SRVs to open at predetermined pressures and specified flow rates. The SRVs will close when pressure drops below 96% of their opening pressure. For the ADAPT-MELCOR model, each of the SRVs is set up to fail open. The valve can fail open due to a per-demand failure probability (high number of cycles) or due to a set number of cycles above 1,000 K (high temperature cycles).

To determine the Cdf for the per-demand failure to close probability Equation 2 was used (Kaplan et al. 1981):

$$P(n) = 1 - (1 - P_d)^n \quad (2)$$

where $P(n)$ = Cdf value (0 to 1); P_d = the per-demand probability for failure to close; and n = number of valve cycles.

Figure 9 shows the resulting Cdf with an assumed per-demand failure probability of $P_d = 0.0027$. The results reported in this study only reflect the 5% probability which corresponds to 19 valve cycles.

The other SRV failure mode, high temperature cycling, is assumed to have the SRV stick to the valve's backseat when steam flow temperature is greater than 1,000 K. For this failure mode, a uniform Cdf was developed between 1 and 10 valve cycles. The 4%, 49%, and 81% Cdf data points were selected which because these points provide whole numbers. This corresponds to 2, 7, and 9 valve cycles.

3.3 *Containment failure*

Past research and scale model testing has been conducted on reinforced and prestressed concrete containments (USNRC, 2006a; USNRC, 1998; Dameron et al. 1995; USNRC, 1992). Through

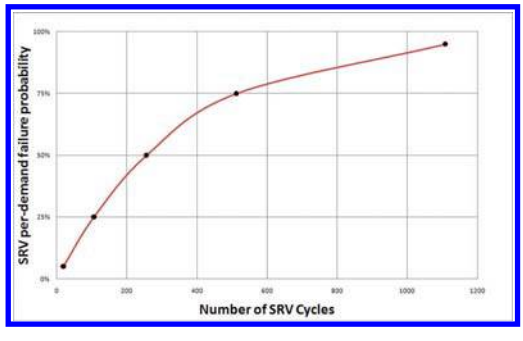

Figure 9. SRV per-demand failure distribution.

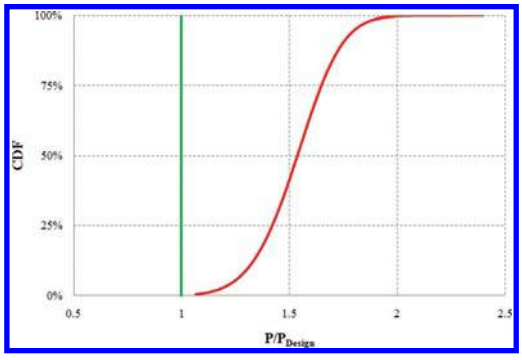

Figure 10. CFC Cdf or containment fragility curve.

this testing, it has been determined that a concrete containment will start to leak before it fails due to rupture. This relationship has been coded into MELCOR.

For this work, two models were used to account for nominal leakage from containment and containment failure. Each model uses a MELCOR flow path adjusted to the containment pressure to accordingly simulate the leakage from containment to the environment. The nominal leak rate is based off a 0.10% containment air volume per day leak rate when pressure reaches containment design pressure. The containment failure model is based off data points collected from NUREG/CR-5121 (USNRC, 1992).

For this work, data obtained from NUREG/CR-6920 (USNRC, 2006b) were used to create a containment failure curve (CFC). The minimum pressure-to-design pressure ratio (P/P_{Design}) for containment failure was taken from NUREG/CR-5121 ($P/P_{Design} = 2.175$) and assumed to correspond 99.99% of the CFC Cdf. This process results in the CFC Cdf (or containment fragility curve) shown in Figure 10. In Figure 10, the red line shows the minimum P/P_{Design} variable which will initiate the containment failure model, and the green line denotes the design pressure ($P/P_{Design} = 1$). For this work, the 5%, 50%, and 95% points on the Cdf were selected. This choice results in a P/P_{Design} of 1.235, 1.536, and 1.803 respectively.

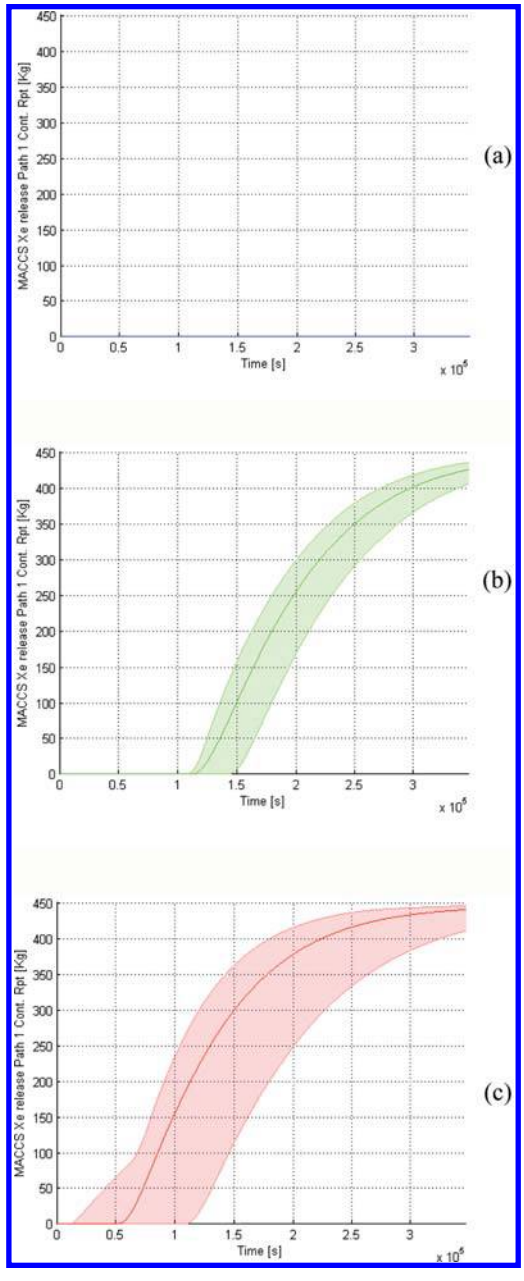

Figure 11. Scenario reduction: (a) power recovery; (b) long-term SBO; (c) short-term SBO.

4 RESULTS

4.1 *Carbon steel creep rupture*

For this work, 436 simulations were produced and clustered with respect to the carbon steel creep rupture distribution. Clustering is based off 15 MELCOR variables including pressures (reactor and containment), temperatures (reactor and hot leg), radionuclide release pathways (containment leakage, rupture, and bypass), creep rupture parameters (carbon steel, stainless steel, and Inconel), containment hydrogen concentrations, and fraction of core melt.

Figure 11 provides the initial clustering for 436 scenarios based on noble gas (Xe) release from

containment as a result of containment rupture using a BW = 23. The clustering of these scenarios are broken down into (a) AC power recovery (Figure 11a), (b) long-term SBO—availability of turbine driven equipment and DC batteries (Figure 11b), and (c) short-term SBO—turbine driven equipment is unavailable (Figure 11c). Figure 11a shows that for power recovery within 28,800 seconds (8 hours), there is no breach of containment and thus no release of noble gases. However, the availability of turbine driven equipment and DC batteries can delay the breach of containment by an average of 57,600 (16 hours). It should be noted that the dark green and red lines shown in Figure 11b and 11c are the representative scenarios for their respective clusters. This representative scenario is the actual scenario that is located closest to the mean of the BW. The shaded areas represent all the other scenarios that fall within the BW.

For the short-term SBO (STSBO) scenarios, the grouping of the SRV failures has some effect on the time to carbon steel creep rupture. Table 1 provides a summary of the creep rupture location (Hot Leg A—HLA, or Hot Leg C—HLC), time to creep rupture, and SRV failure (SRV-A, SRV-B, SRV-C, and SRV-P). Other creep rupture times occurred but those summarized in Table 1 are the only SRV grouping effects that can be determined. The creep rupture parameter had little effect on timing (less than three minutes).

From Figure 11c, the earliest containment ruptures occurred at approximately 12,600 seconds (3.5 hours) into the scenario. They are a result of over pressurization from a high concentration hydrogen deflagration (see Hakobyan et al. 2006 b for a more detailed explanation of hydrogen concentration uncertainties) and a low containment failure probability ($P/P_{Design} = 1.235$).

Figure 12 provides the differences in the reactor coolant system (RCS) pressure profiles for a clustering of (a) STSBO scenarios and (b) long-term SBO (LTSBO) scenarios. As shown in Figure 12b, the RCS pressure profile shows the cooldown until DC batteries are exhausted resulting in the inability to control the turbine driven equipment used for control of make-up water to the steam generators for cooldown. As noted earlier, this cooldown and

Table 1. Carbon steel creep rupture timing and SRV Failure for a STSBO.

Location	Time (hr)	SRV failure
HLC	3.3	A & B & C
HLA or C	3.4	C & (A or B)
HLA	3.45	B & (A or C or P)
HLA	3.62	A & P
HLA	3.66	A

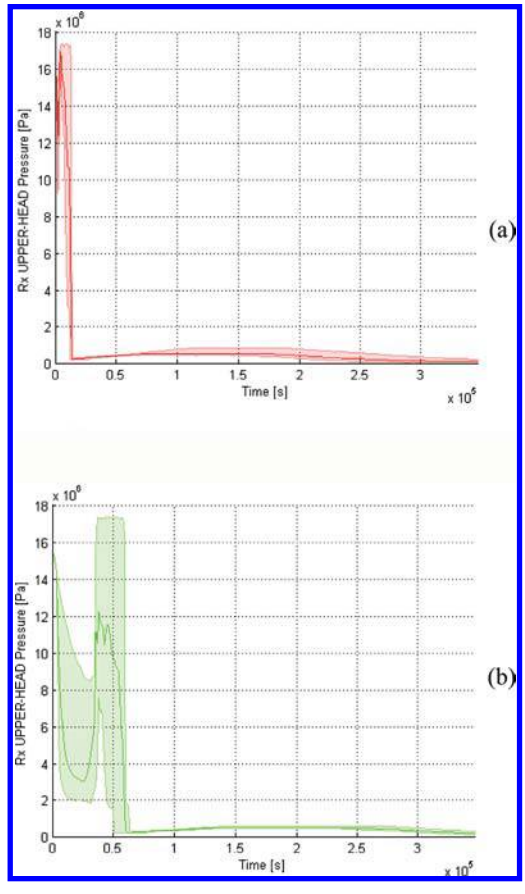

Figure 12. RCS pressure profile: (a) STSBO scenarios, (b) LTSBO scenarios.

subsequent delay in creep rupture further delays breach of containment by an average of 16 hours.

From the observed data of this study for the LTSBO, the timing and grouping of SRV failure had no effect on the timing of the carbon steel creep rupture. Instead, the length of DC battery life and use of turbine driven equipment had the greatest effect on creep rupture timing because of the ability to cooldown the reactor coolant system which prolonged creep rupture. Again, the creep rupture parameter had little effect on timing (less than three minutes).

Both the STSBO and the LTSBO scenarios did not have scenarios in which high temperature SRV cycling occurred.

4.2 *Stainless steel and inconel creep rupture*

The stainless steel creep rupture scenarios produced similar results as those shown in Figure 11 and 12.

However, the timing of creep rupture was delayed by approximately 20 minutes than that of similar scenarios for carbon steel creep rupture. Again, the STSBO SRV sequencing produced similar results for those scenarios shown in Table 1. The LTSBO scenarios were also dependent on DC battery life and use of turbine driven equipment for delaying creep rupture. No scenarios occurred in which high temperature SRV cycling occurred.

No scenarios were produced in which Inconel creep ruptured occurred.

5 CONCLUSIONS

The results analyzed for this dynamic PRA provided insight into the timing of creep rupture and provided some additional detail into the grouping of SRV failures with respect to creep rupture. Currently, work is being done on grouping the 50% and 95% probability distributions for the SRV per demand failure (see Figure 9) which would correspond to 256 and 1108 cycles, respectively. There is a potential of additional SRV failure grouping effects for a STSBO and perhaps a LTSBO. An increased number of SRV cycles may provide data for high temperature SRV cycling as well.

While the uncertainties within the creep rupture parameter did not preclude stainless steel creep rupture occurring before carbon steel creep rupture, the carbon steel creep rupture always occurred before the similar scenario with the same stainless steel creep rupture parameter. Additional analysis needs to be conducted in which prolonged SRV cycling may result in stainless steel creep rupture occurring prior to carbon steel creep rupture for the given creep rupture uncertainty parameters.

Since no Inconel creep ruptures occurred, no timing or sequencing could be conducted. Again, additional investigation into longer SRV per demand failure probabilities may provide insight into Inconel creep rupture.

The post-processing analysis using the 15 MELCOR variables provided clustering based upon power recovery, STSBO, and LTSBO scenarios, and carbon steel and stainless steel creep rupture scenarios. The non-parametric iterative mode-seeking methodology provided the analyst an easy visualization of the clustered scenarios. Furthermore, the representative scenario can provide an actual scenario upon which source term quantification can be based for Level 3 PRA analysis.

REFERENCES

Catalyurek, U., et al., 2010, Development of a Code-Agnostic Computational Infrastructure for the Dynamic Generation of Accident Progression Event Trees, *Reliability Engineering & System Safety*, Volume 95: 278–304.

Dameron, R.A., et al., 1995, Leak area and leakage rate prediction for probabilistic risk assessment of concrete containments under severe core conditions, *Nuclear Engineering and Design*, Volume 156: 173–179.

Gauntt, R.O., et al., 2005, MELCOR Computer Code Manuals—NUREG/CR-6119, Vol. 2, Rev. 3 (SAND2005–5713), *U.S. Nuclear Regulatory Commission*, Washington, D.C. USA.

Hakobyan, A., et al., 2006a, Treatment of Uncertainties in Modeling the Failure of Major RCS Components in Severe Accident Analysis, *Transaction of the American Nuclear Society*, Volume 94: 177–179.

Hakobyan, A., et al., 2006b, Treatment of Uncertainties in Modeling Hydrogen Burning in the Containment during Severe Accidents, *Transactions of the American Nuclear Society*, Volume 95: 683–685.

Hakobyan, A., et al., 2008, Dynamic generation of accident progression event trees, *Nuclear Engineering and Design*, Volume 238: 3457–3467.

Kaplan, S., & B.J. Garrick, 1981, On the Quantitative Definition of Risk, *Risk Analysis*, Volume 1. Number 1: 11–27.

Mandelli, D., et al., 2010, Scenario Aggregation and Analysis via Mean-Shift Methodology, *Proceedings for the 2010 International Congress on Advances in Nuclear Power Plants, ICAPP '10*: Paper 10293, San Diego, CA, USA.

Metzroth, K., et al., 2010, Discretization Sensitivity Studies for Dynamic Event Tree Analyses, *Proceedings for the 2010 Probabilistic Safety Assessment and Management, PSAM10*, Seattle, WA, USA.

Rutt, B., et al., 2006, Distributed Dynamic Event Tree Generation for Reliability and Risk Assessment, *International Workshop on Challenges of Large Applications in Distributed Environments (CLADE),* Paris, France.

USNRC, 1992, Experimental Results from Pressure Testing a 1:6-Scale Nuclear Power Plant Containment, NUREG/CR-5121, *U.S. Nuclear Regulatory Commission*, Washington D.C. USA.

USNRC, 1998, Pretest Prediction Analysis and Posttest Correlation of Sizewell-B 1:10 Scale Prestressed Concrete Containment Model Test, NUREG/CR-5671, *U.S. Nuclear Regulatory Commission*, Washington D.C. USA.

USNRC, 2005, Reevaluation of Station Blackout Risk at Nuclear Power Plants—NUREG/CR-6890, *U.S. Nuclear Regulatory Commission*, Washington D.C. USA.

USNRC, 2006a, Containment Integrity Research at Sandia National Laboratories, NUREG/CR-6906, *U.S. Nuclear Regulatory Commission*, Washington D.C. USA.

USNRC, 2006b, Risk-Informed Assessment of Degraded Containment Vessels, NUREG/CR-6920, *U.S. Nuclear Regulatory Commission*, Washington D.C. USA.